

A Novel Jet Model: Magnetically Collimated, Radiation-Pressure Driven Jet

Shun TAKEUCHI,^{1,2} Ken OHSUGA,³ and Shin MINESHIGE¹

¹*Department of Astronomy, Graduate School of Science, Kyoto University, Sakyo-ku, Kyoto 606-8502*

²*Kwasan Observatory, Kyoto University, Yamashina-Ku, Kyoto 607-8471*

³*National Astronomical Observatory of Japan, Osawa, Mitaka, Tokyo 181-8588*

E-mail : shun@kustastro.kyoto-u.ac.jp

(Received 0 0; accepted 0 0)

Abstract

Relativistic jets from compact objects are ubiquitous phenomena in the Universe, but their driving mechanism has been an enigmatic issue over many decades. Two basic models have been extensively discussed: magnetohydrodynamic (MHD) jets and radiation-hydrodynamic (RHD) jets. Currently, the former is more widely accepted, since magnetic field is expected to provide both the acceleration and collimation mechanisms, whereas radiation field cannot collimate outflow. Here, we propose a new type of jets, radiation-magnetohydrodynamic (RMHD) jets, based on our global RMHD simulation of luminous accretion flow onto a black hole shining above the Eddington luminosity. The RMHD jet can be accelerated up to the relativistic speed by the radiation-pressure force and is collimated by the Lorentz force of a magnetic tower, inflated magnetic structure made by toroidal magnetic field lines accumulated around the black hole, though radiation energy greatly dominates over magnetic energy. This magnetic tower is collimated by a geometrically thick accretion flow supported by radiation-pressure force. This type of jet may explain relativistic jets from Galactic microquasars, appearing at high luminosities.

Key words: accretion, accretion disks — black hole physics — magnetohydrodynamics: MHD — radiative transfer — ISM: jets and outflows

1. Introduction

Astrophysical jets, highly collimated, high velocity plasma outflows, are found in many astrophysical objects, including young stellar objects (YSOs), microquasars, active galactic nuclei (AGNs), and gamma-ray bursts (GRBs). Importantly, the jets (except for YSO jets) are, at least, mildly relativistic and sometimes highly relativistic and are collimated with a small opening angle which is only a few degrees. It is widely accepted from the observations that these relativistic jets are associated with accretion flows onto a central compact object, such as black-holes (see review by Mirabel & Rodríguez 1999). Despite a long research history since the 1970's, how to collimate and accelerate astrophysical jets still remains an open question (e.g., Rees 1984; Meier 2003).

There are two models proposed and considered for the driving mechanism of relativistic jets: magnetohydrodynamic (MHD) jets which are driven by the magnetic process (Lovelace 1976; Blandford & Payne 1982; Uchida & Shibata 1985; Hawley & Balbus 2002) and radiation-hydrodynamic (RHD) jets which are driven by the strong radiation-pressure force (Bisnovatyi-Kogan & Blinnikov 1977; Eggum et al. 1988; Sikora et al. 1996; Okuda et al. 2009). The former is very promising, since not only the acceleration but also the collimation can be accounted for, whereas the latter cannot generally explain the collimation. However, we should remark that most of the previous MHD disk-jet simulations assumed that the underlying accretion flows are radiatively inefficient; i.e., low-luminosity accretion flow (Ichimaru 1977; Narayan & Yi 1994). By contrast, radiation field dominates the dynamics of luminous (radiation-dominated) accretion flows, from which

highly relativistic jets are occasionally observed, especially in the cases of Galactic microquasars.

Here, we examined the complex interactions between matter, radiation, and magnetic fields in the high-luminosity accretion flow and jet, based on our global radiation-magnetohydrodynamic (RMHD) simulations. Our goal is to give good physical explanation why and how relativistic jets can be produced in luminous accretion flows and what kinds of roles magnetic field plays in the situations that radiation field dominates over matter and magnetic energy.

2. Overview of the RMHD Simulations

We analyzed the RMHD simulation data of Ohsuga et al. (2009). Here, we outline the numerical method. We extended the resistive MHD simulations performed by Kato et al. (2004), and solved the equations including the radiation transfer terms numerically in a 2.5-dimensional domain. We used cylindrical coordinates (r, θ, z) , where r , θ , and z are the radial distance, the azimuthal angle, and the vertical distance, respectively. The basic equations are the continuity equation,

$$\frac{\partial \rho}{\partial t} + \nabla \cdot (\rho \mathbf{v}) = 0, \quad (1)$$

the equations of motion,

$$\begin{aligned} \frac{\partial(\rho \mathbf{v})}{\partial t} + \nabla \cdot \left(\rho \mathbf{v} \mathbf{v} - \frac{\mathbf{B} \mathbf{B}}{4\pi} \right) \\ = -\nabla \left(p_{\text{gas}} + \frac{|\mathbf{B}|^2}{8\pi} \right) + \frac{\chi}{c} \mathbf{F}_0 - \rho \nabla \psi_{\text{PN}}, \end{aligned} \quad (2)$$

the energy equation of the gas,

$$\begin{aligned} \frac{\partial e}{\partial t} + \nabla \cdot (e\mathbf{v}) \\ = -p_{\text{gas}} \nabla \cdot \mathbf{v} + \frac{4\pi}{c^2} \eta_a J^2 - 4\pi\kappa B_{\text{bb}} + c\kappa E_0, \end{aligned} \quad (3)$$

the energy equation of the radiation,

$$\begin{aligned} \frac{\partial E_0}{\partial t} + \nabla \cdot (E_0 \mathbf{v}) \\ = -\nabla \cdot \mathbf{F}_0 - \nabla \mathbf{v} : \mathbf{P}_0 + 4\pi\kappa B_{\text{bb}} - c\kappa E_0, \end{aligned} \quad (4)$$

and the induction equation,

$$\frac{\partial \mathbf{B}}{\partial t} = \nabla \times \left(\mathbf{v} \times \mathbf{B} - \frac{4\pi}{c} \eta_a \mathbf{J} \right). \quad (5)$$

Here, ρ is the gas mass density, $\mathbf{v} = (v_r, v_\phi, v_z)$ is the flow velocity, c is the speed of light, e is the internal energy density of the gas, p_{gas} is the gas-pressure, $\mathbf{B} = (B_r, B_\phi, B_z)$ is the magnetic field, $\mathbf{J} (= c\nabla \times \mathbf{B}/4\pi)$ is the electric current, B_{bb} is the blackbody intensity, E_0 is the radiation energy density, \mathbf{F}_0 is the radiative flux, \mathbf{P}_0 is the radiation-pressure tensor, κ is the absorption opacity, and χ is the total opacity, respectively. We adopted anomalous resistivity, η_a (Yokoyama & Shibata 1994), the flux-limited diffusion (FLD) approximation to evaluate \mathbf{F}_0 and \mathbf{P}_0 (Levermore & Pomraning 1981), and the pseudo-Newtonian potential, ψ_{PN} , to incorporate the general relativistic effects, given by $\psi_{\text{PN}} = -GM_{\text{BH}}/(\sqrt{r^2 + z^2} - r_s)$ (Paczynski & Wiita 1980). Here, $r_s (= 2GM_{\text{BH}}/c^2)$ represents the Schwarzschild radius, where G is the gravitational constant and M_{BH} is the mass of the black hole. As the equation of state, we use the relation, $p_{\text{gas}} = (\gamma - 1)e = \rho k_B T_{\text{gas}}/\mu m_p$, where γ is the specific heat ratio, k_B is the Boltzmann constant, T_{gas} is the temperature of the gas, μ the mean molecular weight, and m_p is the proton mass, respectively.

The computational domain is $3r_s \leq r \leq 103r_s$ and $0 \leq z \leq 91.6r_s$. The grid spacing of the radial distance, Δr , and the vertical distance, Δz , is uniform ($\Delta r = \Delta z = 0.2r_s$). The reflection symmetry relative to the equatorial plane (with $z = 0$) is assumed. Free boundary conditions for matter and a magnetic field are adopted; i.e., the matter can freely go out, but cannot to come in, and the magnetic field cannot change across the boundaries. Radiation is set to go out of the boundaries with the radiative flux of cE_0 , except at the innermost boundary at $r = 3r_s$ and $z > 3r_s$, through which no radiation can go out. We also set a non-rotating stellar-mass black hole ($M_{\text{BH}} = 10M_\odot$) at the origin, and initially put a rotating torus at radii around $40r_s$ threaded with closed poloidal magnetic field (plasma- $\beta \equiv p_{\text{gas}}/p_{\text{mag}} = 100$), and a non-rotating isothermal corona. Here, $p_{\text{mag}} (= B^2/8\pi)$ is magnetic pressure force.

3. RMHD Jet Emerging from a Luminous Accretion Flow

In Figure 1, we show a bird's-eye view of luminous accretion flow (at the center, with the brown color), outflow (with the white and the blue color), and the associated magnetic field lines (with the white lines). In the jet region only the parts with high velocities ($\sim 0.6c - 0.7c$) are illustrated by the blue color. The emergence of a magnetic tower formed by the accumulation of the toroidal magnetic field which emerged from the underlying accretion flow is evident. This is quite reminiscent of non-radiative MHD jets (Lynden-Bell 1996; Kato

et al. 2004; Nakamura et al. 2006), in spite of large radiation energy density which by far exceeds the magnetic energy in the present case (discussed later). From the simulation data, we obtain the following quantities; the mass-outflow rate is $\dot{M}_{\text{out}} \sim 10L_E/c^2$; the photon luminosity is $L_{\text{ph}} \sim L_E$; the kinetic luminosity is $L_{\text{kin}} \sim 0.1L_E$; the Poynting luminosity is $L_{\text{poyn}} \sim 0.01L_E$. Note that the Eddington luminosity (L_E) can be exceeded in the case of disk accretion onto black holes because of significant anisotropy of the radiation field and photon trapping effects (Ohsuga & Mineshige 2007). The mass-accretion rate to the central black hole is $\dot{M}_{\text{acc}} \sim 100L_E/c^2$, that exceeds the critical rate giving rise to the Eddington luminosity, on the order of $10L_E/c^2$, i.e., the simulated flow is supercritical (Shakura & Sunyaev 1973; Abramowicz et al. 1988; see Chap. 10 of Kato et al. 2008 for a review). Here, the mass-accretion rate and the mass-outflow rate are calculated by summing up the mass passing through the inner boundary and the upper boundary per unit time with higher velocities than the escape velocity. Photon luminosity, kinetic luminosity, and Poynting luminosity are calculated based on the radiative flux, the kinetic energy, and magnetic energy at the upper boundary.

3.1. Acceleration Mechanism of RMHD Jet

To see what force is responsible for the acceleration of the jet, we evaluate the time-averaged strengths of the vertical components of the gravitational force, the gas-pressure force, the radiation-pressure force, and the Lorentz force at a radius, $r = 10r_s$, and display them in the left panel of Figure 2 as functions of the vertical coordinate, z . This figure unambiguously shows that the RMHD jet is accelerated by the radiation-pressure force (indicated by the red line), and that the Lorentz force (indicated by the blue line) does not contribute much to the acceleration. This is a natural consequence, since the radiation energy density greatly exceeds the magnetic energy density, typically, by more than one order of magnitude. To understand the direction of the radiation-pressure force, we display in the left wall surface of Figure 1 the color contours of the zz -component of the radiation-pressure tensor, P_0^{zz} , overlaid with the radiation-pressure force vectors (arrows), $\chi \mathbf{F}_0/\rho c$, on the meridional plane. We can clearly see that the vertical, outward component of the radiation-pressure force dominates in the jet region (around the z -axis), since the radiation energy density rapidly varies in the vertical direction, but not so much in the horizontal direction; that is, the significant anisotropy of the radiation field (Ohsuga & Mineshige 2007).

3.2. Collimation Mechanism of RMHD Jet

Next, we examine the collimation mechanism of the RMHD jet in the same manner as we did for the acceleration mechanism. We calculate the time-averaged strengths of the radial components of the gravitational force, gas-pressure force, centrifugal force, radiation-pressure force, and the Lorentz force at $z = 40r_s$, and display them in the right panel of Figure 2 as functions of r . In contrast with the left panel, the Lorentz force (indicated by blue solid line) dominates; i.e., the magnetic force works as the a collimation force in the RMHD jet against the outward (centrifugal) force (indicated by the magenta dashed line). We note that magnetic-pressure force and the tension force are comparable. To understand the direction

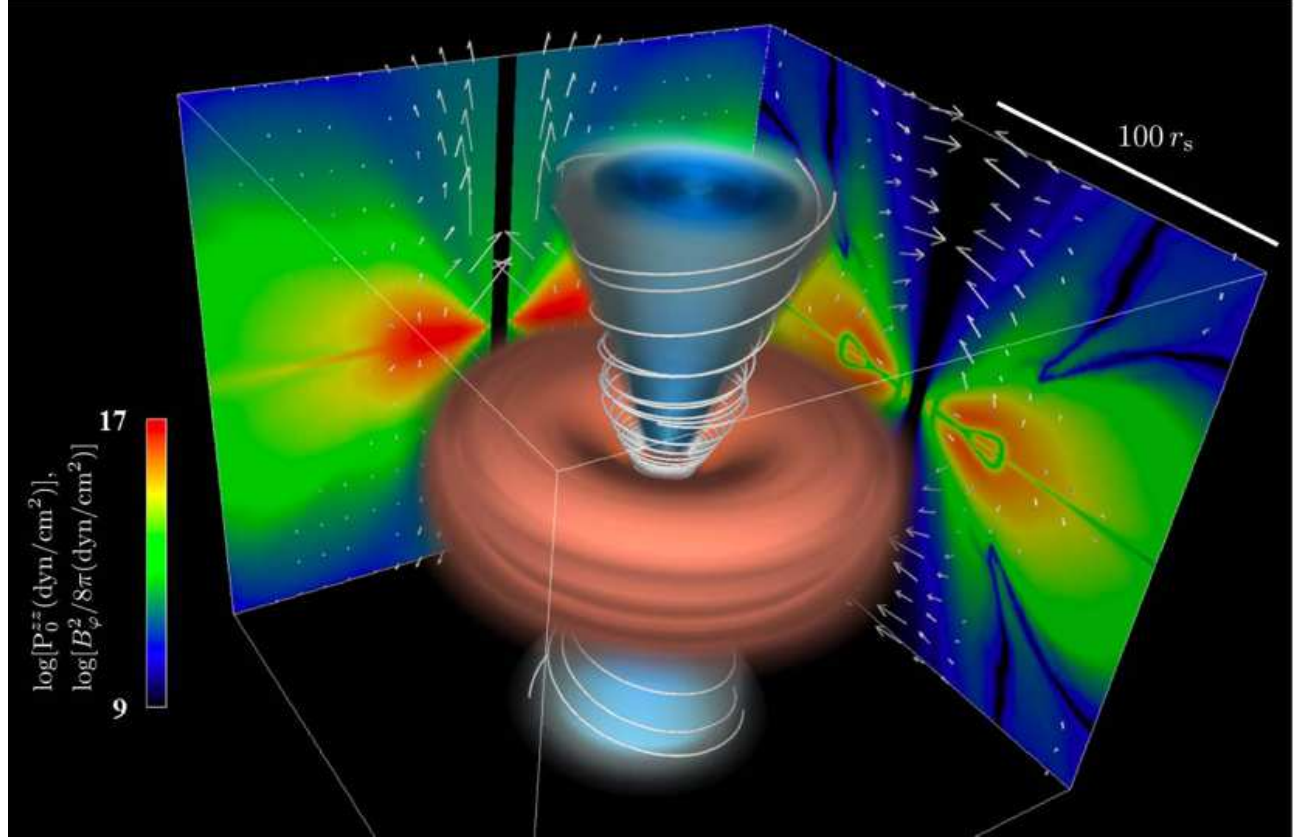


Fig. 1. Bird's-eye view of the luminous accretion flow and the associated RMHD jet. The accretion flow (the gas mass density, brown) and the RMHD jet in which velocities exceed the escape velocity (the velocity, white, blue) are plotted. The high-speed jet ($\sim 0.6c - 0.7c$) is represented by blue. White lines indicate the magnetic field lines. The zz -component of the radiation-pressure tensor (color), P_0^{zz} , overlaid with the radiation-pressure force vectors (arrows) on the meridional plane is projected on the left wall surface, while the magnetic pressure from the azimuthal component of the magnetic field (color), $B_\phi^2/8\pi$, overlaid with the Lorentz force vectors (arrows) on the meridional plane is projected on the right wall surface. The color bar corresponds to the logarithmic value of P_0^{zz} and $B_\phi^2/8\pi$. The arrows on each wall are displayed only in the region in which their values are larger than 10^{10} dyn/g. Each quantity is time-averaged over 1 s, which corresponds to the accretion timescale at several tens of the Schwarzschild radius (r_s).

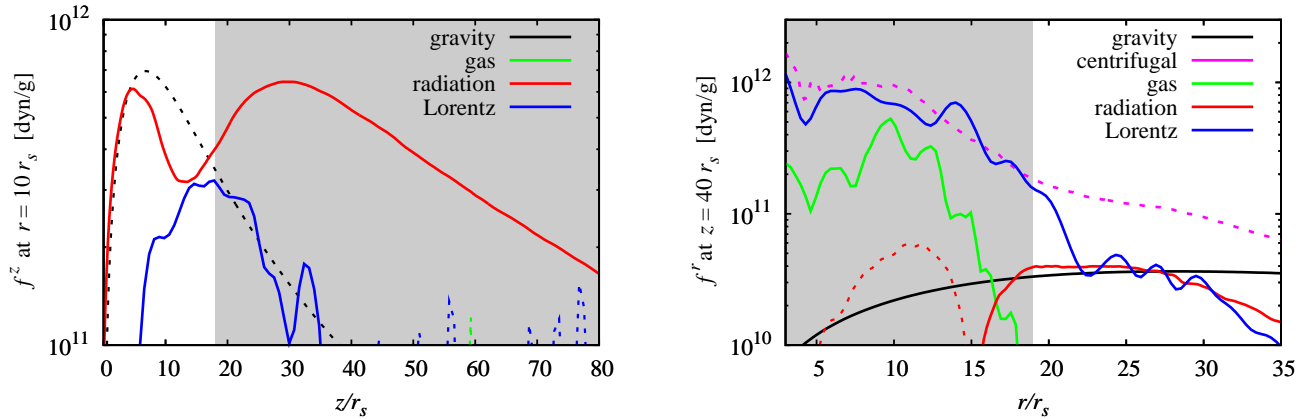


Fig. 2. Acceleration and collimation mechanism of the RMHD jet. Left panel: The vertical profiles of the gravitational force (black), the gas-pressure force (green), the radiation-pressure force (red), and the Lorentz force (blue) at $r = 10 r_s$. The solid lines and the dashed lines indicate the outward force and the inward force, respectively. The radiation-pressure force is responsible for the jet acceleration. Right panel: The radial profiles of the gravitational force (black), the centrifugal force (magenta), the gas-pressure force (green), the radiation-pressure force (red), and the Lorentz force (blue), at $z = 40 r_s$. The solid lines and the dashed lines indicate the inward force and the outward force. We understand that the Lorentz force is responsible for the collimation of the jet. In both panels each quantity is time-averaged over 1 s, and the shadowed areas indicate the jet region in which the outflow velocity exceeds the escape velocity.

of the Lorentz force in each region, we display in the right wall surface of Figure 1 the color contours of the magnetic pressure from the azimuthal component of the magnetic field, $B_\phi^2/8\pi$, overlaid with the Lorentz force vectors (arrows), $\mathbf{J} \times \mathbf{B}/\rho c$, of the RMHD flow on the meridional plane.

As we already mentioned, the radial, inward component of the Lorentz force, i.e., pinch effect of the magnetic field, dominates over other forces, including the radiation-pressure force, in the jet region. This seems, at first glance, odd, since the magnetic energy density is much less than the radiation energy density; say, by a factor of ~ 20 at $(r, z) = (18 r_s, 40 r_s)$. Nevertheless, magnetic force can dominate over the radiation force, since the radiation-pressure force is largely attenuated in the horizontal direction (in the disk plane) because of highly anisotropic distribution of radiation energy. In the high luminosity flow with large matter column density, the accumulation of material around the black hole is responsible for generating rather flat distribution of the radiation energy density in the horizontal direction. As a result, the horizontal component of the radiation-pressure force, which is proportional to the horizontal gradient of the radiation energy density, is largely reduced. By contrast, magnetic energy density shows high concentration ("magnetic tower") in the cylindrical region surrounding the black hole, asserting large inward magnetic force at the inner surface of the magnetic tower. The magnitude of the Lorentz force can be by ~ 5 times as large as that of the radiation force there.

Note that a magnetic field is by nature intrinsically expansive. Thus, there must be something to prevent the field from expanding sideways, thereby decollimating the whole configuration (Uzdensky & MacFadyen 2006; Spruit 2010). In our simulations, it is the geometrically thick accretion flow supported by strong radiation pressure force that prevents the field from expansion. We can prove this by looking at Figure 2 (right) that the central region (the magnetic tower) is confined by the combination of the radiation pressure force (the red curve) and the gravitational force (the black line). Cautions should be taken for the bird's eye view in Figure 1; it only traces very high density regions ("core" of the accretion flow) and substantial amount of material exists around the magnetic tower, as is illustrated in the left wall in Figure 1.

We started the simulations from the particular initial conditions, and we admit that our results may depend on them. We need further simulation studies starting from different initial magnetic field configurations (Igumenshchev et al. 2003; Beckwith et al. 2009). Cases of continuous addition of a magnetic field in a flow should also be necessary to be examined (McKinney & Narayan 2007). We are planning such simulations in future work.

4. Discussion

Recently, Fender et al. (2004) compiled the X-ray observational data of Galactic microquasars in the luminosity-hardness ratio diagram and reported evolutionary paths in the diagram. Importantly, they found a common condition for the occurrence of relativistic jets in microquasars; that is, relativistic jets only appear when the source exhibits a hard-to-soft transition at high luminosities. The typical photon luminosities (L_{ph}), at which

relativistic jets are observed, are close to (or, at least, a few tens of percents of) L_E . Our results are consistent with such observational facts.

The present RMHD simulation, however, does not produce highly relativistic jet with the bulk Lorentz factor of a few. This is partly because our simulations are restricted to the Newtonian dynamics. In future relativistic RMHD simulations will be able to show really relativistic jets by extracting energy from the black hole spin energy. Recently made general relativistic MHD simulations can indeed achieve high Lorentz factor of jets (Blandford & Znajek 1977; Koide et al. 2002; McKinney 2006), though radiation processes are not considered in their simulations. In this sense, our simulations are more relevant to mildly relativistic, persistent jets from a peculiar source, SS433. In fact supercritical accretion is indicated in this source by number of observations (Margon et al. 1979; Kotani et al. 1996; Fabrika 2004).

To conclude, complex interaction between matter, radiation, and magnetic field would be an important factor for the relativistic jet formation at high luminosities. Although radiation energy dominates, magnetic fields manifest themselves in the form of magnetic tower structure, which provides a collimation mechanism, which radiation field cannot give. Such situations are expected to always occur at above 10% of the Eddington luminosity, above which the radiation energy density exceeds, or is at least comparable to, internal gas energy density, and thus exceeds the magnetic energy density. Our global RMHD simulations demonstrate the universal role of magnetic field, as well as the importance of radiation-hydrodynamics in physics of black hole accretion disks and flows.

We would like to thank K. Shibata and Y. Kato for useful comments and discussions. This work is supported in part by the Grant-in-Aid of MEXT (19340044, SM), and by the Grant-in-Aid for the global COE programs on "The Next Generation of Physics, Spun from Diversity and Emergence" from MEXT (SM), Ministry of Education, Culture, Sports, Science, and Technology (MEXT) Young Scientist (B) 20740115 (KO). Numerical computations were in part carried out on Cray XT4 at Center for Computational Astrophysics, CfCA, of National Astronomical Observatory of Japan.

References

- Abramowicz, M. A., Czerny, B., Lasota, J. P., & Szuszkiewicz, E. 1988, *ApJ*, 332, 646
- Beckwith, K., Hawley, J. F., & Krolik, J. H. 2009, *ApJ*, 707, 428
- Bisnovatyi-Kogan, G. S., & Blinnikov, S. I. 1977, *A&A*, 59, 111
- Blandford, R. D., & Znajek, R. L. 1977, *MNRAS*, 179, 433
- Blandford, R. D., & Payne, D. G. 1982, *MNRAS*, 199, 883
- Eggum, G. E., Coroniti, F. V., & Katz, J. I. 1988, *ApJ*, 330, 142
- Fabrika, S. 2004, *Astrophys. Space Phys. Rev.*, 12, 1
- Fender, R. P., Belloni, T. M., & Gallo, E. 2004, *MNRAS*, 355, 1105
- Hawley, J. F., & Balbus, S. A. 2002, *ApJ*, 573, 738
- Ichimaru, S. 1977, *ApJ*, 214, 840
- Igumenshchev, I. V., Narayan, R., & Abramowicz, M. A. 2003, *ApJ*, 592, 1042
- Kato, Y., Mineshige, S., & Shibata, K. 2004, *ApJ*, 605, 307
- Kato, S., Fukue, J., & Mineshige, S. 2008, *Black-Hole Accretion Disks: Towards a New Paradigm* (Kyoto: Kyoto University Press)

- Koide, S., Shibata, K., Kudoh, T., & Meier, D. L. 2002, *Science*, 295, 1688
- Kotani, T., Kawai, N., Matsuoka, M., & Brinkmann, W. 1996, *PASJ*, 48, 619
- Levermore, C. D., & Pomraning, G. C. 1981, *ApJ*, 248, 321
- Lovelace, R. V. E. 1976, *Nature*, 262, 649
- Lynden-Bell, D. 1996, *MNRAS*, 279, 389
- Margon, B., Ford, H.C., Grandi, S.A., & Stone, R.P.S. 1979, *ApJL*, 233, L63
- McKinney, J. C. 2006, *MNRAS*, 368, 1561
- McKinney, J. C., & Narayan, R. 2007, *MNRAS*, 375, 513
- Meier, D. L. 2003, *New Astron. Rev.*, 47, 667
- Mirabel, I. F., & Rodríguez, L. F. 1999, *ARA&A*, 37, 409
- Nakamura, M., Li, H., & Li, S. 2006, *ApJ*, 652, 1059
- Narayan, R., & Yi, I. 1994, *ApJ*, 428, L13
- Ohsuga, K., & Mineshige, S. 2007, *ApJ*, 670, 1283
- Ohsuga, K., Mineshige, S., Mori, M., & Kato, Y. 2009, *PASJ*, 61, L7
- Okuda, T., Lipunova, G. V., & Molteni, D. 2009, *MNRAS*, 398, 1668
- Paczynski, B., & Wiita, P.J. 1980, *A&A*, 88, 23
- Rees, M. L. 1984, *ARA&A*, 22, 471
- Shakura, N. I., & Sunyaev, R. A. 1973, *A&A*, 24, 337
- Sikora, M., Sol, H., Begelman, M. C., & Madejski, G. M. 1996, *MNRAS*, 280, 781
- Spruit, H. C. 2010, *Lecture Notes in Physics*, Berlin Springer Verlag, 794, 233
- Uchida, Y., & Shibata, K. 1985, *PASJ*, 37, 515
- Uzdensky, D. A., & MacFadyen, A. I. 2006, *ApJ*, 647, 1192
- Yokoyama, T., & Shibata, K. 1994, *ApJ*, 436, L197